Carbohydrate Polymers 110 (2014) 518–527

Contents lists available at ScienceDirect

Carbohydrate Polymers

journal homepage: www.elsevier.com/locate/carbpol

# Lead removal onto cross-linked low molecular weight chitosan pyruvic acid derivatives

Peter Osei Boamah[a,b], Qi Zhang[a,c,*], Mingqing Hua[a], Yan Huang[a], Yun Liu[a], Wei Wang[a], Yuanyuan Liu[a]

[a] School of Chemistry and Chemical Engineering, Jiangsu University, Zhenjiang 212013, China
[b] Department of Ecological Agriculture, Bolgatanga Polytechnic, Bolgatanga, Ghana
[c] Hainan Provincial Key Lab of Fine Chemistry, Hainan University, Haikou 570228, China

ARTICLE INFO

*Article history:*
Received 21 January 2014
Received in revised form 21 February 2014
Accepted 5 March 2014
Available online 27 March 2014

*Keywords:*
Water pollution
Lead removal
Low molecular weight chitosan
Pyruvic acid
Factorial design

ABSTRACT

Adsorption capacity of cross-linked low molecular weight chitosan pyruvic acid derivatives $CS_n$PA-GLA ($n = 8, 11$) were examined by employing $2^3$ factorial design method. Three (3) factors and two (2) levels of adsorbent dose (A) (0.05 and 0.1 g), adsorbent type (B) ($CS_8$PA-GLA and $CS_{11}$PA-GLA) and concentration of lead solution (C) (1 and 3 mg/L) were considered. From the statistical analysis, all the main parameters (A, B and C) and some interactions of the main parameters (AC and ABC) had influence on the adsorption process at 5% significance level. The adsorption process was greatly influenced by the adsorbent type (B). The adsorption equilibrium results correlated well with the Freundlich isotherm model. The adsorption kinetic data also correlated well with the pseudo second order. The thermodynamic studies also revealed that the nature of lead adsorption was spontaneous and endothermic. The findings suggest that $CS_8$PA-GLA is better than $CS_{11}$PA-GLA for lead sorption.



## 1. Introduction

Removal of lead from the environment has received needed awareness due to their toxicity, carcinogenicity and other adverse effects (Wu et al., 2013). Wastewater from industries such as metallurgical alloying, glass, battery, mining, printing, ammunition, ceramics, among others (Eren, 2009; Li et al., 2012) are the major sources of lead contamination. Precipitation, complexation, reverse osmosis, ion-exchange, adsorption, among others are techniques employed for heavy metal elimination. Among the aforementioned techniques, adsorption has been identified as a striking process because of its effectiveness and easiness in use for the elimination of metal ions (Sreńscek-Nazzal, Kamińska, Michalkiewicz, & Koren, 2013). Commercial activated carbon is microporous in nature and has excellent adsorption capacity and surface area. This makes it a good material for the elimination of metal ions, however, the high operational cost cannot be overlooked. Consequently, inexpensive adsorbents are attracting the spotlight of numerous experiments for the elimination of metal ions. Among these inexpensive adsorbents, the most admired for the elimination of metal ions is chitosan (Kavianinia, Plieger, Kandile, & Harding, 2012; Rajic et al., 2010). Structurally, chitosan has hydroxyl and amino groups which is good for metal ions sorption. Again, the source and experimental condition of the preparation of chitosan determines its adsorption capacity (Orrego et al., 2010). The adsorption properties of chitosan could be improved via physical or chemical process, and the chemical process includes cross-linking, carboxymethylation, hydroxylation, sulfonation, quaternarization among others. In the midst of the derivatives, modification of chitosan with carboxylic groups has been considered often as a fascinating process for escalating the adsorption capacity of chitosan (Ma, Wang, Zhao, & Tian, 2012). Many researchers have modified chitosan with carboxylic groups to obtain carboxymethyl chitosan (CMC), but modification of different low molecular weight chitosans with pyruvic acid (PA) has not been done so far. CMC has multi-functional groups such as —OH, $—NH_2$, —COOH and makes it exhibit higher affinity for metal ions (Wang, Qin, Ding, Peng, & Wang, 2010). On the other hand, CMC is soluble in pH $\leq$ 7, so it is necessary to cross-link it with glutaraldehyde to make it insoluble in acidic solution and water.

In this study, chitosan was degraded into two kinds of low molecular weight chitosan ($CS_8$ and $CS_{11}$), modified with pyruvic acid (PA) and then cross-linked with glutaraldehyde (GLA) to obtain $CS_8$PA-GLA and $CS_{11}$PA-GLA. In order to evaluate the importance of adsorbent dosage, adsorbent type and Pb (II) concentration, $2^3$ full

* Corresponding author at: School of Chemistry and Chemical Engineering, Jiangsu University, Zhenjiang 212013, China. Tel.: +86 0511 82611886; fax: +86 0511 88791800.
*E-mail addresses:* qzhang@ujs.edu.cn, ujshxhg001@yahoo.com (Q. Zhang).

http://dx.doi.org/10.1016/j.carbpol.2014.03.034
0144-8617/

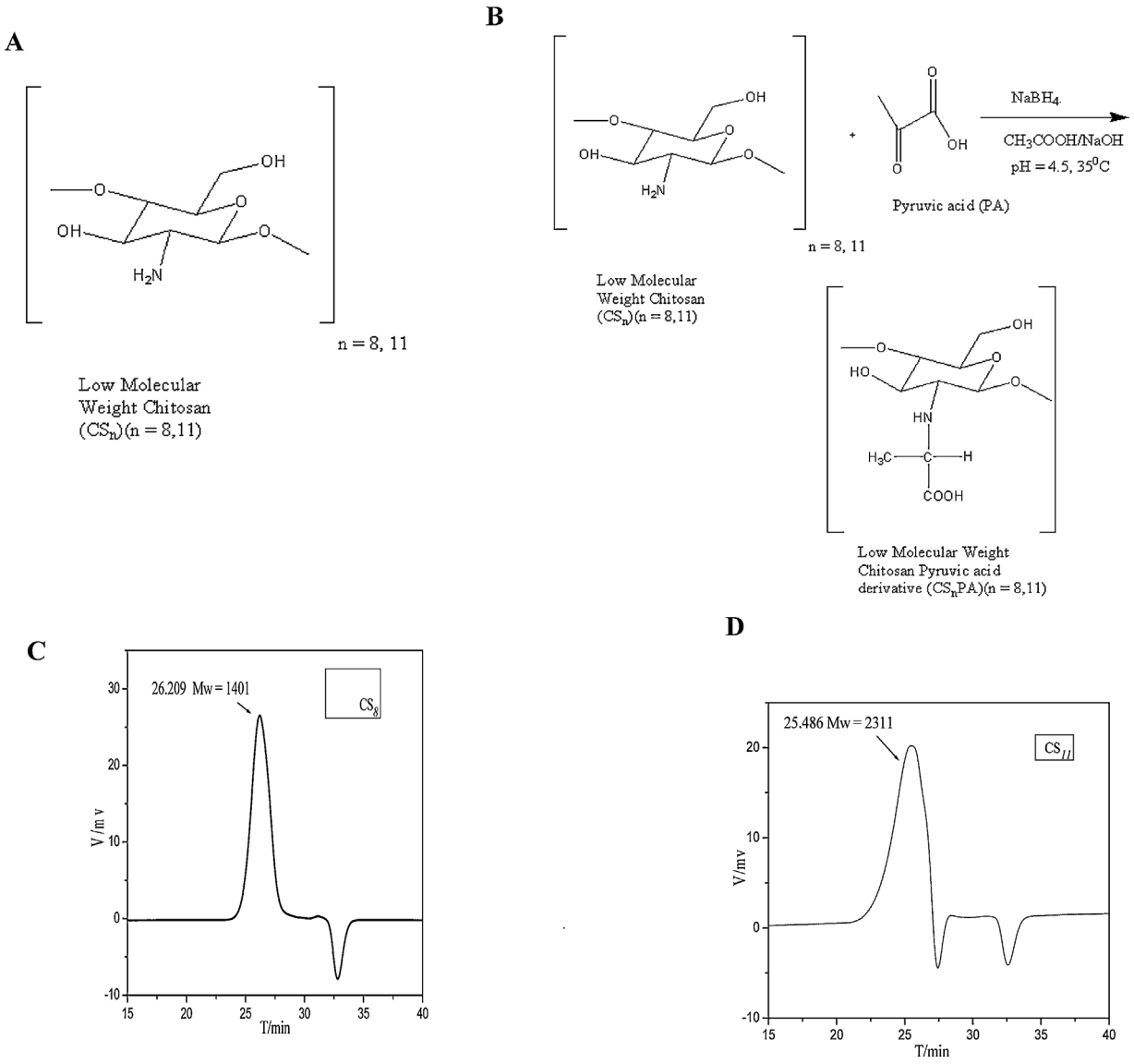


**Fig. 1.** Structure of low molecular weight chitosan ($CS_n$) ($n = 8, 11$) (A); modification of low molecular weight chitosan ($CS_n$) ($n = 8, 11$) with pyruvic acid (PA) (B); size exclusion chromatography (SEC) of $CS_8$ (C); size exclusion chromatography (SEC) of $CS_{11}$ (D).

factorial design was used. Factorial design was used to cut down the overall research cost, the number of experiments and time. Also, it was used to determine which main factors or combined factors effects were statistical significant for the elimination of lead ions and how a factor varied according to the level of the other factors.

## 2. Materials and methods

### 2.1. Materials

Chitosan (CS) (molecular weight = 200 kDa Degree of deacetylation = 95%) was purchased from Sinopharm Chemical Reagent Co., Ltd. (Shanghai, China), hydrogen peroxide, pyruvic acid (PA), glutaraldehyde (GLA) and all other chemicals and reagents were of analytical grade. Distilled water was used to prepare solutions.

### 2.2. Preparation of low molecular weight chitosan ($CS_n$) ($n = 8, 11$) using microwave

The method from our laboratory was employed in the preparation of low molecular weight chitosan (Zhang, 2009). 2 g of chitosan (CS) was weighed and placed in a three mouth flask (250 mL). 160 mL of 0.5% aqueous acetic acid was added and mechanically stirred for 10 min. 4 mL of $H_2O_2$ (30%) was dropped slowly, and the mixture was agitated mechanically for 2–3 min. Degradation at 90 °C, 600 W for 30 and 50 min were done to obtain $CS_{11}$ and $CS_8$ respectively using microwave. The solution pH was attuned to neutral using KOH solution (2 M) at 25 °C, and insoluble impurities were removed by vacuum filtration. The solution was evaporated to a proper amount in a single flask (250 mL) with a rotary evaporator and precipitated with anhydrous ethanol. A vacuum oven was used to dry the low molecular weight chitosan ($CS_n$) ($n = 8, 11$) at 30 °C after filtration and washed with anhydrous ethanol. The structure of low molecular weight chitosan ($CS_n$) ($n = 8, 11$) is shown in Fig. 1A.

### 2.3. Modification of low molecular weight chitosan ($CS_n$) ($n = 8, 11$) with pyruvic acid (PA)

20 mL of 0.20 M acetic acid was added to 1 g of $CS_n$ ($n = 8, 11$). Ten drops of acetic acid (99.5%) and 70 mL of methanol were added afterwards. Pyruvic acid (2.825 g) dissolved in 10 mL of methanol

was added over a period of 5 min at 35 °C. The slurry was stirred for 1 h after which the pH was attuned to 4.5 using NaOH (2 M). $NaBH_4$ (1.5 g) was dropped slowly, and the solution was mechanically stirred for 24 h. Hydrochloric acid (2 M) was used to attune the pH to 4.5. It was evaporated and then filtered by adding anhydrous methanol. $CS_nPA$ ($n$ = 8, 11) was vacuum dried at 30 °C. The modification of low molecular weight chitosan ($CS_n$) ($n$ = 8, 11) with pyruvic acid (PA) is shown in Fig. 1B.

### 2.4. Cross linking of $CS_nPA$ ($n$ = 8, 11) with glutaraldehyde (GLA)

0.5 g of $CS_nPA$ ($n$ = 8, 11) was swelled in 20 mL of methanol and 5 drops of acetic acid (99.5%) was added. Glutaraldehyde (GLA) (0.537 g) was dropped slowly and was agitated at 25 °C for a day. $CS_nPA$-GLA ($n$ = 8, 11) was washed with methanol through filtration and vacuum dried at 30 °C.

### 2.5. Characterization

$CS_n$ ($n$ = 8, 11) molecular weights were known by employing the method from our laboratory (Huang et al., 2012). The molecular weights of $CS_n$ ($n$ = 8, 11) were determined through size exclusion chromatography (SEC) using an RI K-2301 refractive index detector and TSK-GEL G4000 PWXL column (30 cm × 7.5 mm). The solute was eluted with HAc/$NH_4$Ac buffer solution (pH 4.5) at a flow rate of 0.43 mL $min^{-1}$. Fourier transform infrared spectroscopy (FTIR) (Nicolet Nexus 470, USA) was also used to characterize $CS_n$, $CS_nPA$ and $CS_nPA$-GLA (where $n$ = 8, 11) before and after adsorption of lead.

### 2.6. Standard Pb (II) solution

Lead stock solution (1000 mg/L) was prepared from $Pb(NO_3)_2$ (analytical grade). The stock solution was diluted to obtain the desired Pb (II) concentrations. Concentrations prior as well as subsequent to adsorption were estimated by Atomic Absorption Spectrometer (AAS) (TAS-986, China).

### 2.7. Adsorption experiment

A batch experiment was done to ascertain adsorbent dosage, adsorbent type and lead concentration influence on the removal of lead ions onto $CS_nPA$-GLA ($n$ = 8, 11), and to examine combined effect of those parameters using $2^3$ factorial design. The factors as well as their high (+) and low (−) levels are presented in Table 1A. In each trial, weighted amount of adsorbent (0.05 or 0.1 g) was placed in a flask with 25 mL of Pb (II) concentration (1 or 3 mg/L). The solution (pH 5) (potassium hydrogen phthalate/sodium hydroxide buffer) was agitated at 200 rpm at a temperature of 50 °C. After 4 h, filtration was done and the lead ion concentration was analyzed using AAS. Adsorption experiment was done in duplicate and the average was taken.

For the adsorption isotherm results, 0.05 g of adsorbent was placed in a flask with 25 mL of varying initial concentration of Pb (II) (1–5 mg/L). Five mg/L concentration of lead with change in time (1–5 h) was monitored for the kinetic studies, and the thermodynamic studies were also done at 40 and 50 °C.

Eq. (1) was used to compute the adsorption capacity ($q_e$)

$$q_e = \frac{C_i - C_e}{W} \cdot V \quad (1)$$

$C_i$ is the initial lead (II) concentration measured in mg/L, $C_e$ is the final lead (II) concentration measured in mg/L, $V$ is the Pb (II) ions volume measured in L; $W$ is the dosage of $CS_nPA$-GLA ($n$ = 8, 11) in g.

**Table 1**
Factors and levels for the $2^3$ factorial design (A); design matrix and the results of the $2^3$ full factorial design (B); estimated effects and coefficients for $q_e$ (mg/g) (C); analysis of variance for $q_e$ (mg/g) (D).

A

| Factors | Low level (−1) | High level (+1) |
|---|---|---|
| Adsorbent dosage (A) (g) | 0.05 | 0.1 |
| Adsorbent type (B) | $CS_8$PA-GLA | $CS_{11}$PA-GLA |
| Pb(II) concentration (C) (mg/L) | 1 | 3 |

B

| Experiment | A | B | C | Adsorption capacity ($q_e$) (mg/g) |
|---|---|---|---|---|
| 1 | + | + | + | 0.001 |
| 2 | + | − | − | 0.195 |
| 3 | − | − | − | 0.336 |
| 4 | + | + | − | 0.004 |
| 5 | − | + | − | 0.088 |
| 6 | − | + | + | 0.034 |
| 7 | − | − | + | 0.223 |
| 8 | + | − | + | 0.202 |

C

| Term | Effect | Coefficient | SE coeff. | Standardized effect ($T$) | $P$-value |
|---|---|---|---|---|---|
| Constant | | 0.1354 | 0.003435 | 39.41 | 0.000 |
| A | −0.0698 | −0.0349 | 0.003435 | −10.15 | 0.000 |
| B | −0.2073 | −0.1036 | 0.003435 | −30.17 | 0.000 |
| C | −0.0407 | −0.0204 | 0.003435 | −5.93 | 0.000 |
| AB | 0.0112 | 0.0056 | 0.003435 | 1.64 | 0.140 |
| AC | 0.0428 | 0.0214 | 0.003435 | 6.22 | 0.000 |
| BC | 0.0122 | 0.0061 | 0.003435 | 1.78 | 0.112 |
| ABC | −0.0172 | −0.0086 | 0.003435 | −2.51 | 0.036 |

D

| Source | DF | Seq SS | Adj SS | Adj MS | $F$-value | $P$-value |
|---|---|---|---|---|---|---|
| Main effects | 3 | 0.197913 | 0.197913 | 0.065971 | 349.40 | 0.000 |
| 2-Way interactions | 3 | 0.008417 | 0.008417 | 0.002806 | 14.86 | 0.001 |
| 3-Way interactions | 1 | 0.001190 | 0.001190 | 0.001190 | 6.30 | 0.036 |
| Residual error | 8 | 0.001510 | 0.001510 | 0.000189 | | |
| Pure error | 8 | 0.001510 | 0.001510 | 0.000189 | | |
| Total | 15 | 0.209030 | | | | |

$S$ = 0.0137409, $R$-Sq = 99.28%, $R$-Sq (adj) = 98.65%. *Note*: SE coeff., standard error coefficient; S, standard error; $R$-Sq, $R$ squared; $R$-Sq (adj), $R$ squared adjusted; DF, degrees of freedom; Seq SS, sequential sum of squares; Adj SS, adjusted sum of squares; Adj MS, adjusted mean square.

### 2.8. The factorial design

Based on preliminary studies, two levels and three factors were chosen. Table 1B shows the layout of the factorial experiment. The experiment was randomized to avoid consistent biases and the data were analyzed with Minitab version 16. The principal factors and combined factors effects were also determined.

## 3. Results and discussion

### 3.1. Characterization

Chitosan (CS) (Mw = 200 kDa, DD = 95%) was degraded into $CS_8$ and $CS_{11}$. Fig. 1C and D shows the size exclusion chromatography (SEC) of $CS_8$ and $CS_{11}$. The SEC equipment determined the average molecular weight of the degraded chitosan to be 1401 and 2311 Da respectively, and the maximum signal intensity was 26.209 and 25.486 mV respectively. This shows that chitosan (CS) was successfully degraded into $CS_8$ and $CS_{11}$.

The functional groups —$NH_2$ and —OH found in chitosan are good for metal ions complexation, and the introduction of pyruvic acid into the two kinds of low molecular weight chitosan was to improve

its sorption ability for metal ions. In addition, cross-linking of $CS_8$PA and $CS_{11}$PA with glutaraldehyde was also to enhance the mechanical strength and chemical resistance (Ngah & Fatinathan, 2008; Wan Ngah, Endud, & Mayanar, 2002). Fig. 2A and B shows the FTIR spectra of $CS_8$, $CS_8$PA, $CS_8$PA-GLA and $CS_{11}$, $CS_{11}$PA, $CS_{11}$PA-GLA respectively. The most important bands for $CS_8$ and $CS_{11}$ respectively can be ascribed as follows: 3370.15 and 3357.13 $cm^{-1}$ (—OH and —$NH_2$ group stretching vibrations), 2928.60 and 2928.06 $cm^{-1}$ (—CH stretch in —CH as well as $CH_2$), 1596.52 and 1592.85 $cm^{-1}$ ($NH_2$ bending vibration), 1385.04 and 1405.36 $cm^{-1}$ (—CH symmetric bending vibrations in —CHOH—), 1073.30 and 1073.15 $cm^{-1}$ (—CO stretch in —COH—) (Rajiv Gandhi, Kousalya, Viswanathan, & Meenakshi, 2011). Subsequent to the modification of $CS_8$ and $CS_{11}$ with pyruvic acid, there appeared a unique band belonging to —COOH at 1731.56 and 1728.68 $cm^{-1}$ respectively. This means that it is easy to modify chitosan with pyruvic acid when the molecular weight decreases (Cao, Yuan, Lin, Yin, & Tu, 2008). In addition, $CS_8$PA and $CS_{11}$PA were cross-linked with glutaraldehyde (GLA), and a peak appeared at 1631, and 1635.25 $cm^{-1}$ respectively showing that low molecular weight chitosan pyruvic acid derivatives were successfully crossed-linked with glutaraldehyde. More importantly, the band related to the carboxylic group at 1731.56 $cm^{-1}$ shifted to 1737 $cm^{-1}$ and at 1728.68 $cm^{-1}$ shifted to 1733.68 $cm^{-1}$ for $CS_8$PA and $CS_{11}$PA respectively after the cross linking reaction.

Fig. 2C depicts FTIR spectra of $CS_8$PA-GLA + Pb (II) and $CS_{11}$PA-GLA + Pb (II). From Fig. 2C, strong bands observed at 3370 $cm^{-1}$, and 3357 $cm^{-1}$ for $CS_8$ and $CS_{11}$ respectively reduced. Other changes were observed at 1596, 1592 and 1385, 1405 $cm^{-1}$ for $CS_8$ and $CS_{11}$ respectively. This wavenumber was assigned to bending and deformation of the nitrogen (N) and hydrogen (H) bonding which confirms that N found in chitosan is good for lead (II) ion attachment (Ngah & Fatinathan, 2010). Again, band related to the carboxylic group at 1737 and 1733.68 $cm^{-1}$ for $CS_8$PA-GLA and $CS_{11}$PA-GLA respectively disappeared after the adsorption process, indicating the involvement of —COOH in the adsorption process.

### 3.2. Factorial design

Factorial plots were employed to assess adsorbent dosage, adsorbent type and lead (II) concentration effect on the adsorption capacity of $CS_8$PA-GLA and $CS_{11}$PA-GLA. Fig. 3A illustrates cube plot for adsorption capacity of the three factors. In order to ascertain the significant effect of the main factors and the interactions on $q_e$, analysis of variance and *P*-value were used. Pareto chart plots were also used to authenticate the main effect and interactions effect on $q_e$.

### 3.3. ANOVA

Estimated effects, coefficients, standard error of each coefficient, and analysis of variance for the design are shown in Table 1C and D. In order to estimate the significance of the regression coefficients, Student's *t*-test was employed. At 95% confidence level, all effects were significant except AB and BC and the model offered a good $R^2$ (adjusted) value of 98.65%. Lead adsorption capacity by $CS_8$PA-GLA and $CS_{11}$PA-GLA was then expressed as

$$q_e = 0.1354 - 0.0349A - 0.1036B - 0.0204C + 0.0214AC - 0.0086ABC \quad (2)$$

This equation shows how the experimental factors and their interactions affect Pb (II) ions sorption (Sjöblom & Creaser, 2008). The factors and their interactions effect on the adsorption capacity followed the order: adsorbent type (B) > adsorbent dosage (A) > adsorbent dosage-concentration interaction (AC) > concentration(C) > adsorbent dosage- adsorbent type-concentration interaction (ABC). From Eq. (2), it can be noticed that all the main factors A, B and C had a negative effect on $q_e$, which means that an increase of these factors (A, B and C) led to a decreased $q_e$. On the other hand, a positive value of the interaction effect (AC) means an increase in adsorption capacity (Baccouche, Ennouri, Felfoul, & Attia, 2013). The highest value of $q_e$ was obtained at the lowest levels of adsorbent dosage, adsorbent type, and concentration of Pb (II).

ANOVA for $q_e$ is shown in Table 1D. From the analysis, at 95% confidence level, the studied parameters, adsorbent dosage (A), adsorbent type (B), and concentration of Pb (II) (C) and their interaction AC and ABC were statistically significant to $q_e$ while AB and BC were not statistically significant.

### 3.4. The main factors effects

Fig. 3B shows the main effect plots for lead removal. Adsorbent type (B) was the most significant factor for the adsorption process because it had the longest vertical line (Kuram & Ozcelik, 2013). From the coefficient as shown in Eq. (2), adsorbent type was negative which meant that lead removal was not favored at high adsorbent type level. Also, increasing the adsorbent type level from $CS_8$PA-GLA to $CS_{11}$PA-GLA at both low and high levels of adsorbent dosage (A) and Pb (II) concentration (C) decreased the adsorption capacity by 0.248 mg/g and 0.201 mg/g respectively. Thus, the intermolecular distance of $CS_8$PA-GLA was smaller than $CS_{11}$PA-GLA, and that resulted in the former having higher adsorption capacity than the latter because small intermolecular distance facilitates intermolecular interactions(Manzoor, Nadeem, Iqbal, Saeed, & Ansari, 2013).

The second important main effect was the effect of adsorbent dosage (A). It was seen that as adsorbent dosage increases from 0.05 to 0.1 g at both low and high levels of adsorbent type (B) and Pb (II) concentration (C), the adsorption capacity decreased by 0.14 mg/g and 0.033 mg/g respectively. This decrease in adsorption capacity was as a result of the increase in the number of unsaturated adsorption sites as adsorbent dosage increases (Manzoor et al., 2013).

The next essential main factor was the effect of Pb (II) concentration(C). As Pb (II) concentration (C) increases from 1 to 3 mg/L at both low and high levels of adsorbent dosage (A) and adsorbent type (B), there was a decrease in adsorption capacity by 0.113 mg/g and 0.003 mg/g respectively. At 1 mg/L, the ratio of active sites to initial Pb (II) ions was larger, hence the higher adsorption capacity. On the other hand, at 3 mg/L, the numbers of metal ions were comparatively higher than the accessible sorption sites and this resulted in lower adsorption capacity (Saadat & Karimi-Jashni, 2011).

### 3.5. The interaction effects

Fig. 3C shows the plots for interaction effects. An interaction is considered significant when the lines are not parallel (Baccouche et al., 2013). From Fig. 3C, interactions of adsorbent dosage and Pb (II) concentration (AC), and adsorbent dosage, adsorbent type and Pb (II) concentration (ABC) of the main factors were statistically significant in determining $q_e$ while interactions of adsorbent dosage and adsorbent type (AB) and adsorbent type and Pb (II) concentration (BC) were not significant.

### 3.6. Student's t-test

In order to establish whether the calculated effects were significantly different from zero, Student's *t*-test was carried out, and

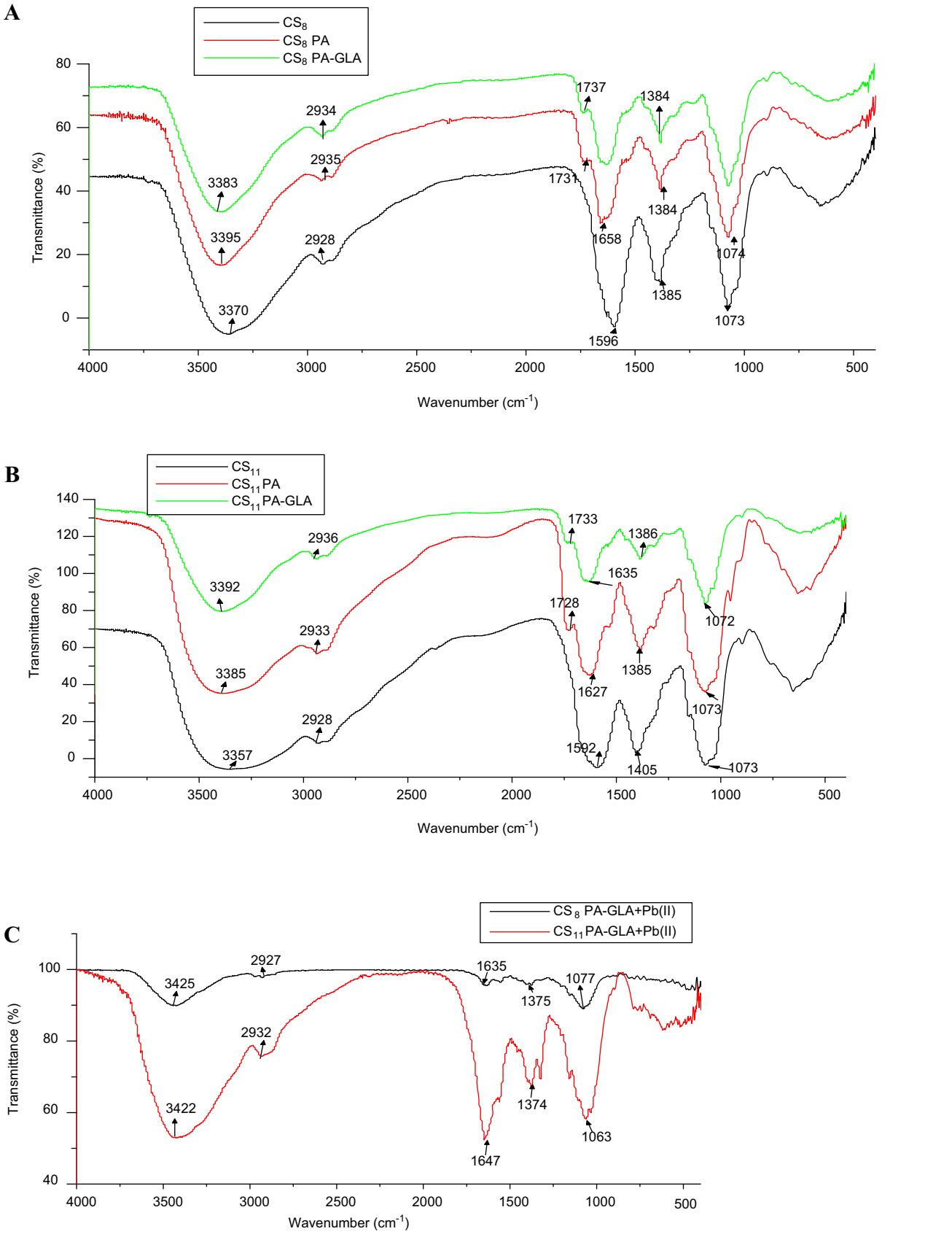


**Fig. 2.** FTIR spectra of $CS_8$, $CS_8$PA and $CS_8$PA-GLA (A); FTIR spectra of $CS_{11}$, $CS_{11}$PA and $CS_{11}$PA-GLA (B); FTIR spectra of $CS_8$PA-GLA and $CS_{11}$PA-GLA after the adsorption of Pb (II) ions (C).

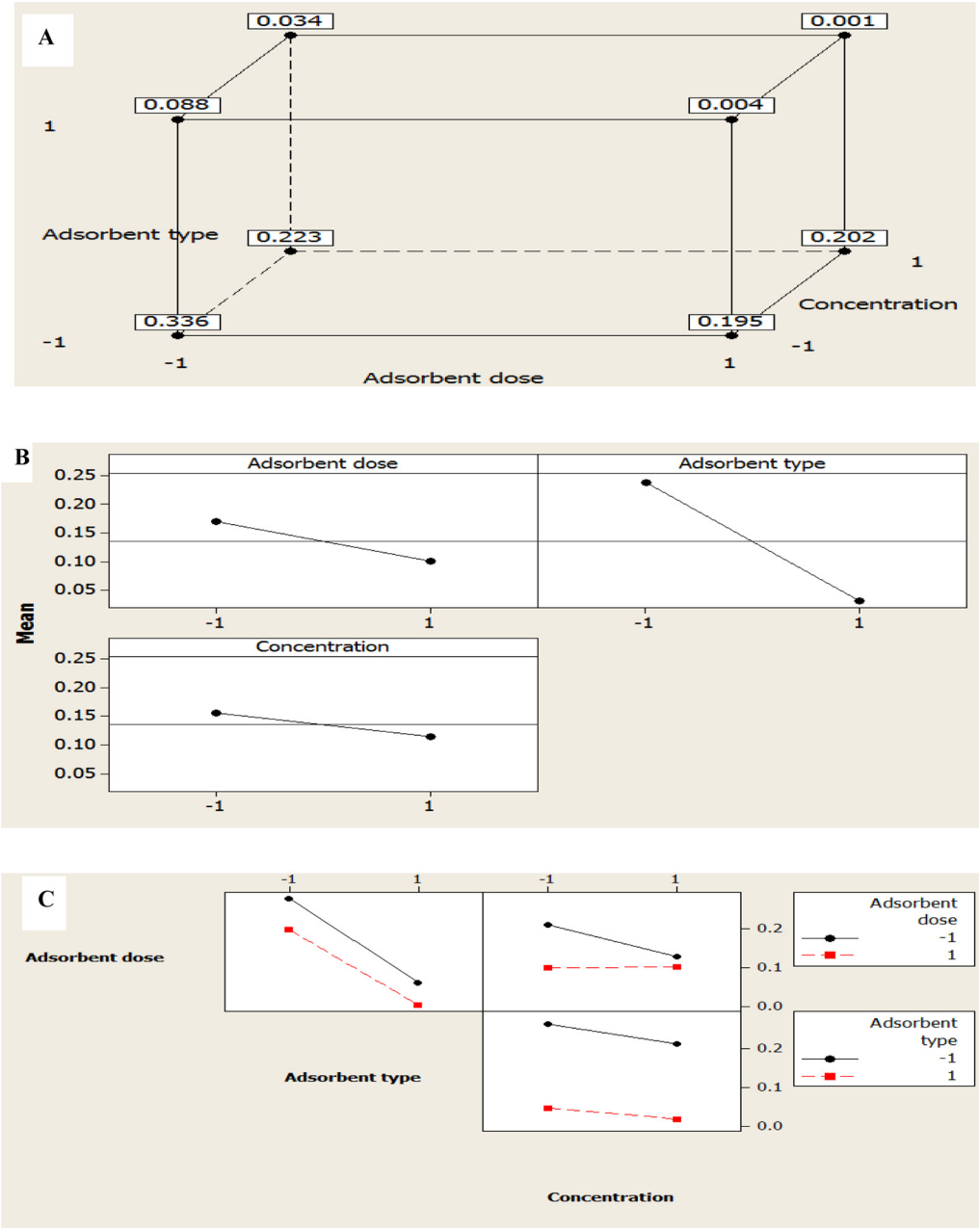


**Fig. 3.** Cube plots for $q_e$ (A); main effects plot for $q_e$ (B); interaction effects plot for $q_e$ (C).

these values are depicted in a Pareto chart (Fig. 4A). At 95% confidence level and eight (8) DF, the value of $t$ was read as 2.31 and a vertical line called the reference line was drawn to show minimum statistical significance. The bars (B, A, AC, C, and ABC) that exceeded the reference line at 95% confidence interval were considered as significant. The other bars (BC and AB) that remained inside the reference line were considered as not significant (Baccouche et al., 2013).

### 3.7. Normal probability plots

Fig. 4B shows normal probability plot of standardized effects and the plot is fully consistent with all the analysis done to test for significant results. Square signs were used to depict statistically significant effects while circle signs depicted insignificant effects (Saadat & Karimi-Jashni, 2011).

### 3.8. Adsorption isotherms

This study considered the Langmuir, Freundlich and Temkin models (Jayakumar, Gomathi, & Sudha, 2013). The Langmuir model is given as:

$$\frac{1}{q_e} = \frac{1}{Q^0} + \frac{1}{bQ^0C_e} \quad (3)$$

$C_e$ is the equilibrium concentration measured in mg/L, $q_e$ is the quantity of lead ion adsorbed measured in mg/g at equilibrium, $Q^0$ is the maximum adsorption capacity measured in mg/g, $b$ is the adsorption energy measured in L/mg.

The capacity of adsorption and adsorption energy was estimated from the gradient and intercept respectively of $1/q_e$ vs. $1/C_e$ plot (plot not displayed).

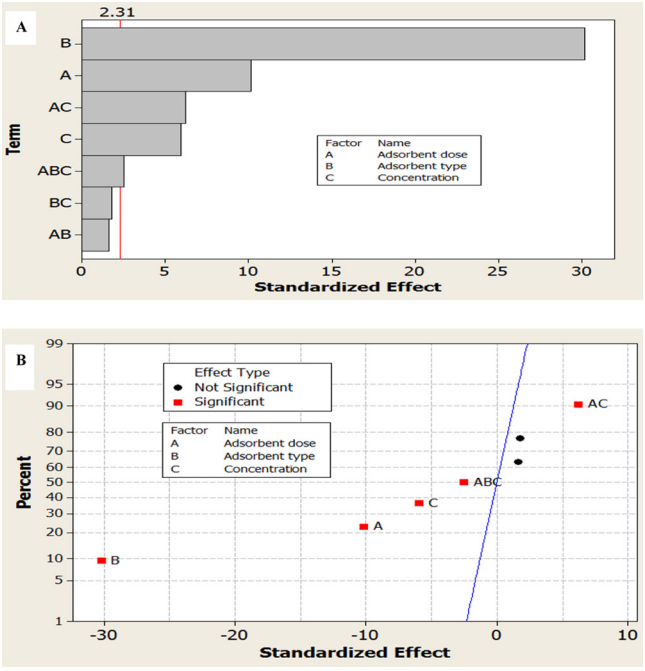


**Fig. 4.** Pareto chart of the standardized effects (A); normal probability plot of standardized effects (B).

The Freundlich model is given as:

$$\log\ q_e = \log K_F + \left(\frac{1}{n}\right) \log\ C_e \tag{4}$$

$q_e$ is the amount of lead adsorbed in mg/g of adsorbent, $C_e$ is the concentration of lead ions in mg/L at equilibrium, $K_F$ is the capacity of adsorption (mg/g), and $1/n$ is the intensity of adsorption. The capacity of adsorption and intensity of adsorption was estimated from the gradient and intercept respectively of $\log q_e$ against $\log C_e$ plot (Fig. 5A and B).

The Temkin isotherm model is given as:

$$q_e = a_t + 2.303 b_t\ \log\ C_e \tag{5}$$

$a_t$ is the adsorption capacity measured in mg/g, $b_t$ is the intensity of adsorption measured in L/mg. The adsorption capacity and intensity was estimated from intercept and gradient respectively of $q_e$ vs. $\log C_e$ plot (Fig. 5C and D).

Table 2A shows the equilibrium adsorption data of lead ions onto $CS_8$PA-GLA and $CS_{11}$PA-GLA. From Table 2A, the adsorption capacity ($Q^0$) of $CS_8$PA-GLA was higher than $CS_{11}$PA-GLA from the Langmuir model. This could be due to the molecular weight of $CS_8$PA-GLA since the low molecular weight resulted in high adsorption capacity. This is because small intermolecular distance enhances intermolecular interactions (Zhou, Yang, Guo, & Chen, 2003). The $R^2$ value of Langmuir, Freundlich, Temkin was 0.81, 1.00, 0.95 and 0.67, 1.00, 0.89 for $CS_8$PA-GLA and $CS_{11}$PA-GLA respectively. The values of $R^2$ are regarded as a measure of the goodness-of-fit of experimental data on the isotherm models. The applicability of the three isotherms models for the present study for the adsorbents followed the order: Freundlich > Temkin > Langmuir.

### 3.9. Adsorption kinetics study

The first-order of Lagergren and second-order-pseudo model (Shahtalebi & Mckay, 2011) was used to study the kinetic adsorption of Pb (II) onto $CS_8$PA-GLA and $CS_{11}$PA-GLA.

The equation for the pseudo-first order is given as:

$$\log(q_e - q_t) = \log\ q_e - \frac{k_1 t}{2.303} \tag{6}$$

$q_e$ is the quantity of lead ions adsorbed in mg/g on adsorbent at equilibrium, $q_t$ is the amounts of lead ions adsorbed measured in mg/g on adsorbent at time $t$, $k_1$ is the rate constant measured in $min^{-1}$. The gradient of $\log(q_e - q_t)$ vs. $t$ was used to estimate the value of $k_1$ (Fig. 6A and B).

The pseudo-second order equation is given as:

$$\frac{t}{q_t} = \frac{1}{k_2 q_e^2} + \frac{t}{q_e} \tag{7}$$

$q_e^2$ is the highest adsorption capacity measured in milligram per gram, $k_2$ is the adsorption rate constant measured in g $mg^{-1}$ $min^{-1}$. From the intercept of $t/q_t$ vs. $t$ plot (Fig. 6C and D), $k_2$ value was estimated. Table 2B shows the data for adsorption kinetics studies of Pb (II) onto $CS_8$PA-GLA and $CS_{11}$PA-GLA where the

**Table 2**
Langmuir, Freudlich and Temkin Isotherm constants and correlation coefficients (A); kinetic parameters for Pb (II) adsorption onto $CS_8$PA-GLA and $CS_{11}$PA-GLA (B); thermodynamic parameters for Pb (II) adsorption onto $CS_8$PA-GLA and $CS_{11}$PA-GLA (C).

A

| Adsorbent | Freudlich | | | Langmuir | | | Temkin | | |
|---|---|---|---|---|---|---|---|---|---|
| | $K_F$ (mg/g) | $1/n$ | $R^2$ | $b$ (L/mg) | $Q^0$ (mg/g) | $R^2$ | $a_t$ (mg/g) | $b_t$ (L/mg) | $R^2$ |
| $CS_8$PA-GLA | 0.50 | 0.99 | 1.00 | −4.54 | 0.42 | 0.81 | 0.47 | 1.01 | 0.95 |
| $CS_{11}$PA-GLA | 0.50 | 1.00 | 1.00 | −4.03 | 0.26 | 0.67 | 0.69 | 0.78 | 0.89 |

B

| Adsorbent | Experimental value | Pseudo first order kinetic model | | | Pseudo second order kinetic model | | |
|---|---|---|---|---|---|---|---|
| | $q_{e,exp}$ | $q_e$ (mg/g) | $k_1$ ($min^{-1}$) | $R^2$ | $q_e$ (mg/g) | $k_2$ (g $mg^{-1}$ $min^{-1}$) | $R^2$ |
| $CS_8$PA-GLA | 2.23 | 0.23 | $-9.212 \times 10^{-3}$ | 0.89 | 2.23 | $2.89 \times 10^{-1}$ | 0.999 |
| $CS_{11}$PA-GLA | 2.29 | 2.15 | $9.212 \times 10^{-3}$ | 0.25 | 2.07 | $-9.82 \times 10^{-2}$ | 0.996 |

C

| Adsorbent | Temperature (K) | $\Delta G^\circ$ (kJ $mol^{-1}$) | $\Delta H^\circ$ (kJ $mol^{-1}$) | $\Delta S^\circ$ (kJ $mol^{-1}$ $K^{-1}$) |
|---|---|---|---|---|
| $CS_8$PA-GLA | 313 | −3.379 | 28.99 | 0.103 |
| | 323 | −4.413 | | |
| $CS_{11}$PA-GLA | 313 | −3.739 | 28.97 | 0.104 |
| | 323 | −4.784 | | |

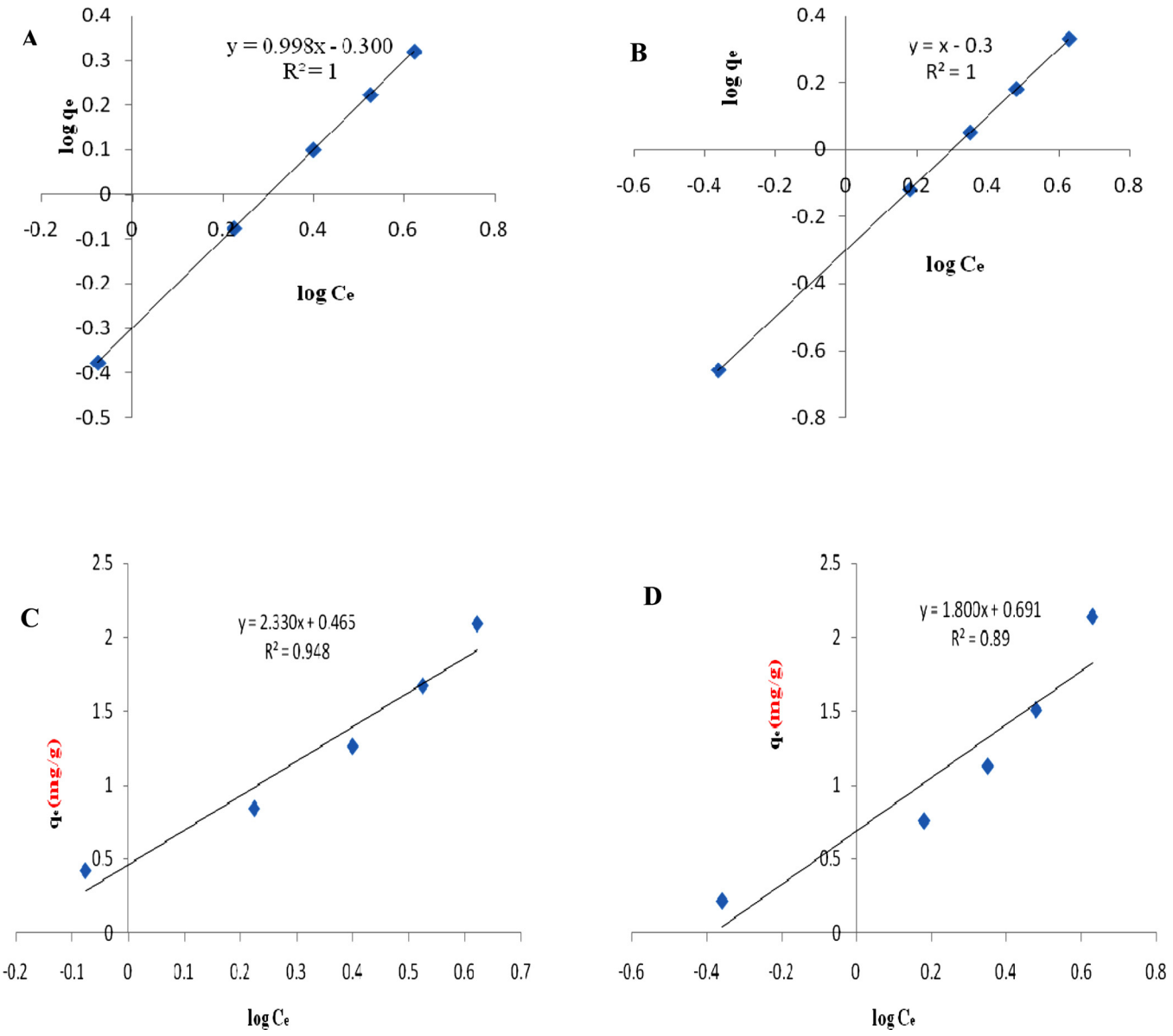


**Fig. 5.** Freundlich plots for adsorption of Pb (II) onto $CS_8$PA-GLA (A); Freundlich plots for adsorption of Pb (II) onto $CS_{11}$PA-GLA (B); Temkin plots for adsorption of Pb (II) onto $CS_8$PA-GLA (C); Temkin plots for adsorption of Pb (II) onto $CS_{11}$PA-GLA (D).

experimental value of $q_e$ correlated very well with the pseudo-second-order equation. The $R^2$ value of the pseudo-second-order equation was 0.999 and 0.996 for $CS_8$PA-GLA and $CS_{11}$PA-GLA respectively which is in agreement with most Pb (II) adsorption experiments (Wan, Kan, Rogel, & Dalida, 2010).

### 3.10. Thermodynamic studies

Pb (II) removal onto $CS_8$PA-GLA and $CS_{11}$PA-GLA were observed at two temperatures (313 and 323 K). Gibbs free energy change ($\Delta G^\circ$), entropy change ($\Delta S^\circ$), equilibrium constant ($K_{eq}$) and enthalpy change ($\Delta H^\circ$) were estimated from the following equations (Cestari, Vieira, de Oliveira, & Bruns, 2007).

$$K_{eq} = \frac{C_o}{C_e} \quad (8)$$

$$\Delta G^\circ = -RT \ln K_{eq} \quad (9)$$

$$\Delta G^\circ = \Delta H^\circ - T\Delta S^\circ \quad (10)$$

$C_0$ is the initial concentration of lead ions removed onto $CS_8$PA-GLA and $CS_{11}$PA-GLA per volume of solution used for this study, $C_e$ is the concentration of lead ions solution at equilibrium, $T$ is the temperature of solution measured in Kelvin, and $R$ is the Universal gas constant.

Table 2C shows the estimated value of thermodynamic parameters for $CS_8$PA-GLA and $CS_{11}$PA-GLA. The sign of the Gibbs free energy change value shows that the adsorption process was quick, and the sign of the entropy change value also shows that the freedom of lead ions was not too restricted in $CS_8$PA-GLA and $CS_{11}$PA-GLA (Rajiv Gandhi et al., 2011). Additionally, the sign of enthalpy change value confirmed the endothermic disposition of the adsorption process.

### 3.11. Pb (II) adsorption mechanism

It is clear from the FTIR data that, lead removal onto $CS_8$PA-GLA and $CS_{11}$PA-GLA was governed by adsorption. There was a shift in the wavenumber for the functional groups: $-NH_2$ and $-OH$, but

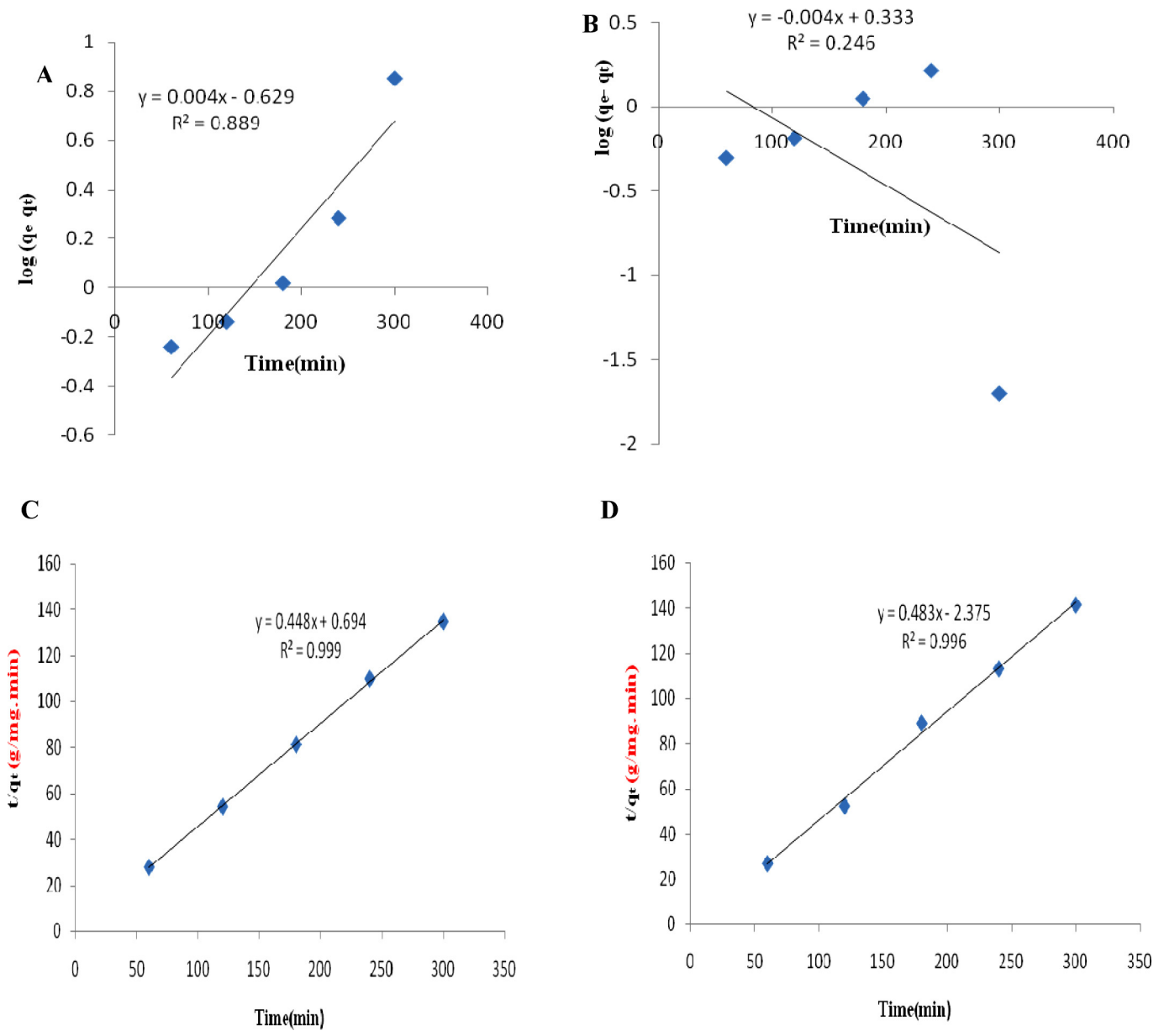


**Fig. 6.** Pseudo first order plots for adsorption of Pb (II) onto $CS_8$PA-GLA (A); pseudo first order plots for adsorption of Pb (II) onto $CS_{11}$PA-GLA (B); pseudo second order plots for adsorption of Pb (II) onto $CS_8$PA-GLA (C); pseudo second order plots for adsorption of Pb (II) onto $CS_{11}$PA-GLA (D).

the band for the —COOH group disappeared after the adsorption process. This shows that $NH_2$, —OH and —COOH groups participated in the adsorption mechanism (Witoon, Permsirivanich, Donphai, Jaree, & Chareonpanich, 2013).

## 4. Conclusions

The adsorption behavior of two prepared adsorbents was examined by employing $2^3$ factorial design method. Three (3) factors and two (2) levels of adsorbent dose (A) (0.05 and 0.1 g), adsorbent type (B) ($CS_8$PA-GLA and $CS_{11}$PA-GLA) and concentration of solution (C) (1 and 3 mg/L) were considered. All the main parameters (A, B and C) and some interactions of the main parameters (AC and ABC) had influence on the adsorption process at 5% significance level. The adsorption process was greatly influenced by the adsorbent type (B). The adsorption equilibrium results were subjected to the isotherm models of Temkin, Freundlich and Langmuir. Freundlich isotherm model for $CS_8$PA-GLA and $CS_{11}$PA-GLA was superior to the others. The adsorption kinetic data also correlated well with the pseudo second order. The thermodynamic studies also revealed that the nature of lead adsorption was spontaneous and endothermic. The findings suggested that, $CS_8$PA-GLA is better than $CS_{11}$PA-GLA for lead sorption.

## References

Baccouche, A., Ennouri, M., Felfoul, I., & Attia, H. (2013). A physical stability study of whey-based prickly pear beverages. *Food Hydrocolloids, 33*, 234–244.

Cao, Y., Yuan, W., Lin, Q., Yin, X. Q., & Tu, W. (2008). Chitosan pyruvic acid derivatives: preparation, moisture absorption–retention ability and antioxidative activity. *Key Engineering Materials, 361*, 963–966.

Cestari, A. R., Vieira, E. F., de Oliveira, I. A., & Bruns, R. E. (2007). The removal of Cu (II) and Co (II) from aqueous solutions using cross-linked chitosan—Evaluation by the factorial design methodology. *Journal of Hazardous Materials, 143*, 8–16.

Eren, E. (2009). Removal of lead ions by Unye (Turkey) bentonite in iron and magnesium oxide-coated forms. *Journal of Hazardous Materials, 165*, 63–70.

Huang, Y., Cao, B., Yang, X., Zhang, Q., Han, X., & Guo, Z. (2012). Gd complexes of diethylenetriaminepentaacetic acid conjugates of low-molecular-weight

chitosan oligosaccharide as a new liver-specific MRI contrast agent. *Magnetic Resonance Imaging*, *31*, 604–609.
Jayakumar, S., Gomathi, T., & Sudha, P. (2013). Sorption studies of lead (II) onto cross linked and non cross linked bio polymeric blends. *International Journal of Biological Macromolecules*, *59*, 165–169.
Kavianinia, I., Plieger, P. G., Kandile, N. G., & Harding, D. R. (2012). Fixed-bed column studies on a modified chitosan hydrogel for detoxification of aqueous solutions from copper (II). *Carbohydrate Polymers*, *90*, 875–886.
Kuram, E., & Ozcelik, B. (2013). Multi-objective optimization using taguchi based grey relational analysis for micro milling of Al 7075 material with ball nose end mill. *Measurement*, *46*, 1849–1864.
Li, T.-t., Liu, Y.-g., Peng, Q.-q., Hu, X.-j., Liao, T., Wang, H., et al. (2012). Removal of lead (II) from aqueous solution with ethylenediamine-modified yeast biomass coated with magnetic chitosan microparticles: Kinetic and equilibrium modeling. *Chemical Engineering Journal*, *214*, 189–197.
Ma, F., Wang, Z., Zhao, H., & Tian, S. (2012). Plasma depolymerization of chitosan in the presence of hydrogen peroxide. *International Journal of Molecular Sciences*, *13*, 7788–7797.
Manzoor, Q., Nadeem, R., Iqbal, M., Saeed, R., & Ansari, T. M. (2013). Organic acids pretreatment effect on Rosa bourbonia phyto-biomass for removal of Pb (II) and Cu (II) from aqueous media. *Bioresource Technology*, *132*, 446–452.
Ngah, W., & Fatinathan, S. (2008). Adsorption of Cu (II) ions in aqueous solution using chitosan beads, chitosan–GLA beads and chitosan–alginate beads. *Chemical Engineering Journal*, *143*, 62–72.
Ngah, W., & Fatinathan, S. (2010). Pb (II) biosorption using chitosan and chitosan derivatives beads: Equilibrium, ion exchange and mechanism studies. *Journal of Environmental Sciences*, *22*, 338–346.
Orrego, C., Salgado, N., Valencia, J., Giraldo, G., Giraldo, O., & Cardona, C. (2010). Novel chitosan membranes as support for lipases immobilization: Characterization aspects. *Carbohydrate Polymers*, *79*, 9–16.
Rajic, N., Stojakovic, D., Jovanovic, M., Logar, N. Z., Mazaj, M., & Kaucic, V. (2010). Removal of nickel (II) ions from aqueous solutions using the natural clinoptilolite and preparation of nano-NiO on the exhausted clinoptilolite. *Applied Surface Science*, *257*, 1524–1532.
Rajiv Gandhi, M., Kousalya, G., Viswanathan, N., & Meenakshi, S. (2011). Sorption behaviour of copper on chemically modified chitosan beads from aqueous solution. *Carbohydrate Polymers*, *83*, 1082–1087.
Saadat, S., & Karimi-Jashni, A. (2011). Optimization of Pb (II) adsorption onto modified walnut shells using factorial design and simplex methodologies. *Chemical Engineering Journal*, *173*, 743–749.
Shahtalebi, A., & Mckay, G. (2011). Modeling batch kinetics of the sorption of copper (II) ions onto pyrolytic tyre char. *Journal of Environmental Science and Engineering*, *5*, 138–145.
Sjöblom, J., & Creaser, D. (2008). Latent variable projections of sensitivity data for experimental screening and kinetic modeling. *Computers & Chemical Engineering*, *32*, 3121–3129.
Sreńscek-Nazzal, J., Kamińska, W., Michalkiewicz, B., & Koren, Z. C. (2013). Production, characterization and methane storage potential of KOH-activated carbon from sugarcane molasses. *Industrial Crops and Products*, *47*, 153–159.
Wan, M.-W., Kan, C.-C., Rogel, B. D., & Dalida, M. L. P. (2010). Adsorption of copper (II) and lead (II) ions from aqueous solution on chitosan-coated sand. *Carbohydrate Polymers*, *80*, 891–899.
Wan Ngah, W., Endud, C., & Mayanar, R. (2002). Removal of copper (II) ions from aqueous solution onto chitosan and cross-linked chitosan beads. *Reactive and Functional Polymers*, *50*, 181–190.
Wang, W., Qin, C., Ding, Y., Peng, H., & Wang, L. (2010). Effect of dietary carboxymethyl chitosans on the levels of iron, zinc and copper in mice. *Carbohydrate Polymers*, *81*, 203–206.
Witoon, T., Permsirivanich, T., Donphai, W., Jaree, A., & Chareonpanich, M. (2013). $CO_2$ hydrogenation to methanol over Cu/ZnO nanocatalysts prepared via a chitosan-assisted co-precipitation method. *Fuel Processing Technology*, *116*, 72–78.
Wu, J., Wang, L., Zhou, J., Zhang, X., Liu, Y., Zhao, X., et al. (2013). Recovery of acetoin from the aqueous solution by means of a novel hyper-cross-linked resin: Equilibrium and kinetics. *Journal of Food Engineering*, *119*, 714–723.
Zhang, Q. (2009). Fluorescence study on the interaction of narrow distribution low polymerization degree chitooligosaccharides and human serum albumin. *Spectroscopy and Spectral Analysis*, *29*, 2523–2526.
Zhou, Y. G., Yang, Y. D., Guo, X. M., & Chen, G. R. (2003). Effect of molecular weight and degree of deacetylation of chitosan on urea adsorption properties of copper chitosan. *Journal of Applied Polymer Science*, *89*, 1520–1523.